
Bias or Optimality? Disentangling Bayesian Inference and Learning Biases in Human Decision-Making

Prakhar Godara

Department of Psychology
New York University

New York, 10003

prakhargodara@gmail.com

Abstract

Recent studies [Palminteri et al., 2017, Lefebvre et al., 2017, den Ouden et al., 2013, Frank et al., 2007, Chambon et al., 2020, Xia et al., 2021] among others claim that human behavior in a two-armed Bernoulli bandit (TABB) task is described by *positivity* and *confirmation* biases, implying that "Humans do not integrate new information objectively." However, we find that even if the agent updates its belief via objective Bayesian inference, fitting the standard Q-learning model with asymmetric learning rates still recovers both biases. Bayesian inference cast as an effective Q-learning algorithm has symmetric, though decreasing, learning rates. We explain this by analyzing the stochastic dynamics of these learning systems using master equations: both confirmation bias and unbiased but decreasing learning rates yield the same behavioral signature—reduced action switching probabilities compared to constant, unbiased updates. Finally, we propose experimental protocols to disentangle true cognitive biases from artifacts of decreasing learning rates.

1 Introduction

Studying human decision-making in idealized experimental settings has been a cornerstone of both behavioral economics Herrmann et al. [2008], Godara et al. [2022], Godara and Herminghaus [2023], Wang et al. [2024], Andreoni and Croson [2008] and cognitive science Steyvers et al. [2009], Zhang and Yu [2013], Wilson et al. [2014], Brown et al. [2022], Wu et al. [2022]. One particularly useful paradigm for such investigations is the N -armed Bernoulli bandit (called TABB when $N = 2$) task Katehakis and Veinott [1987], where participants must balance exploration and exploitation to maximize rewards. Each action (or arm) offers binary outcomes (zero or one) with unknown probabilities, and the subject's goal is to maximize cumulative rewards over T trials.

This task captures the explore-exploit dilemma faced by all decision-makers operating in uncertain environments. Its simplicity has made it a widely studied paradigm in behavioral studies, where researchers explore not only optimal decision strategies but also how real human behavior deviates from this ideal. Recently, the TABB task has also been used to study how people make inferences from stochastic feedback, and research has revealed the presence of cognitive biases in human learning—most notably, positivity and confirmation biases. These biases have repeatedly been observed in adult humans [Palminteri et al., 2017, Lefebvre et al., 2017, den Ouden et al., 2013, Frank et al., 2007, Chambon et al., 2020], adolescents [Xia et al., 2021], rodents [Ohta et al., 2021] and macaques [Farashahi et al., 2019] to name a few. These findings are based on fitting a reinforcement learning framework, Q-learning, to subject behavior data.

Q-learning, which has been linked to dopaminergic activity in the brain Dayan and Abbott [2005], describes how agents update their expectations of reward from chosen and unchosen options based

on the difference between expected and received outcomes. The model can be expressed as:

$$Q_{t+1}^v = Q_t^v + \begin{cases} \alpha_+^v \cdot (r_t^v - Q_t^v), & \text{if } (r_t^v - Q_t^v) > 0 \\ \alpha_-^v \cdot (r_t^v - Q_t^v), & \text{if } (r_t^v - Q_t^v) < 0. \end{cases} \quad (1)$$

where $v \in \{c, u\}$ denotes either the chosen arm (c) or the unchosen arm (u), and r_t^v is the observed reward at time t (corresponding to the v arm). Here we have written the Q-learning in a general manner, accounting for tasks with (called "Experiment-2" in Palminteri et al. [2017]) and without ("Experiment-1") counterfactual information¹. In particular for tasks without counterfactual information we have $\alpha_{\pm}^u = 0$.

The parameters α_+^v (for positive prediction errors) and α_-^v (for negative prediction errors) are learning rates, dictating how quickly the agent adjusts its expectations based on the outcome. Human biases are formalized through these learning rates:

1. Positivity bias: $\alpha_+^c > \alpha_-^c$, i.e. the agent, for the chosen arm, favors positive updates more than negative ones.
2. Confirmation bias: $\alpha_+^c > \alpha_-^c$ and $\alpha_-^u > \alpha_+^u$, i.e. the agent favors positive updates for the chosen arm, but negative updates for the unchosen arm.

However, Q-learning is not the only framework used to model human behavior. Another influential approach is Bayesian inference, in which agents update their beliefs in a statistically optimal manner based on the likelihood of new evidence. Because Bayesian models are often considered the benchmark of rational inference Zellner [1988], they have become central to many cognitive science models of decision-making George and Hawkins [2009], L Griffiths et al. [2008]. While Bayesian inference operates differently from Q-learning, one might naturally expect that if we fit a Q-learning model to data generated by a Bayesian agent, the inferred learning rates would be unbiased—after all, a rational learner should not exhibit systematic distortions. In other words, if our methodology for detecting biases is sound, it should classify Bayesian inference as an unbiased process. Yet, as we will show, this is not the case.

When fitting the Q-learning model to data generated by an agent using Bayesian inference, we still observe the same biases—positivity and confirmation—commonly found in human data. This result raises an important question: are these biases inherent to human cognition, or do they emerge as an artifact of the Q-learning framework used to model behavior?²

In this paper, we demonstrate that the latter is true. In particular we will focus on TABB tasks with counterfactual information as both positivity and confirmation biases are observed in that setup. First, we will reformulate Bayesian inference in terms of Q-learning to establish an equivalent framework. We show that while Bayesian inference leads to unbiased learning, the learning rates decrease over time, which can lead to the appearance of biases when fitting constant learning rate models. Next, we will use the master equation approach Gardiner [1985] to study the stochastic dynamics of these learning systems and provide an explanation for the emergent biases. Finally, we will compare the predictive power of Bayesian models versus Q-learning models in fitting human behavioral data from Palminteri et al. [2017], and propose novel experiments that could help disentangle true cognitive biases from optimal learning mechanisms.

Bayesian inference models

Bayes-greedy and Bayes-optimal behavior in TABB

We begin by describing the Bayes-optimal behavior for the TABB task of a finite horizon T and no counterfactual information. As the rewards corresponding to a single arm (or action) $a = i \in \{1, 2\}$ in TABB are Bernoulli random variables parameterized by p_i , the belief of the agent about the reward rates can be viewed as a probability distribution over possible values of p_i . Assuming that the agent performs Bayesian inference and starts with a uniform prior distribution over $p_i \in [0, 1]$

¹Usually the agents are only informed of the rewards of the chosen arm i.e. no counterfactual information.

²A similar study [Katahira, 2018] studies how a choice autocorrelation can generate pseudo-positivity/confirmation bias. Here we present yet another mechanism that generates such statistical artefacts.

for $i \in \{1, 2\}$, the belief probability distributions can be represented by the two-parameter beta distribution. At any given time t , the belief³ can then be written as

$$b_t = (\alpha_1, \beta_1, \alpha_2, \beta_2) \in \mathbb{N}_0^4 : \alpha_1 + \beta_1 + \alpha_2 + \beta_2 = t, \quad (2)$$

where α_i is the number of (thus far) obtained successes corresponding to pulling the arm $a = i$, and β_i the failures. Here (α_i, β_i) are the parameters of the beta-distribution corresponding to arm $a = i$. We therefore see that in the specific case of TABB, Bayes inference can be viewed as a deterministic update rule

$$b_{t+1} = b_t + y(a_t, r_t), \quad (3)$$

where r_t is the reward obtained at time t for the chosen arm, and y is given by

$$y(a, r) = \begin{cases} (1, 0, 0, 0), & \text{if } a = 1, r = 1, \\ (0, 1, 0, 0), & \text{if } a = 1, r = 0, \\ (0, 0, 1, 0), & \text{if } a = 2, r = 1, \\ (0, 0, 0, 1), & \text{if } a = 2, r = 0. \end{cases}$$

Further, the mean of the beta distribution with parameters (α_i, β_i) is given by $p_i^s = \frac{\alpha_i + 1}{\alpha_i + \beta_i + 2}$. This represents the "average/effective belief" of the agent about the reward of an arm, i.e. the agent effectively believes the reward to be distributed according to a Bernoulli distribution with parameter p_i^s (here s is used to demonstrate that this is the subjective p_i value), i.e., the distribution of rewards under the average belief $b_t(r|a = i) = B(p_i^s)$.

So far we described how the agent updates its beliefs. We now proceed to describe the decision policy $a_t = \pi(b_t)$. The (Bayes-)optimal decision policy π^* is a solution of the Bellman equation as follows⁴.

$$V^*(b_t) = \max_a \sum_r \left[b_t(r|a) (r + \delta(y - y(a, r)) V(b_t + y)) \right], \quad (4)$$

where δ represents the Dirac-delta function, and $\pi^*(b_t) = \arg \max_a V(b_t)$. Notice that in this strategy, we maximize a sum of immediate and future rewards. For tasks with counterfactual information, where the agents are also presented with the evidence of the reward of the unchosen arm, the subsequent belief states become independent of the current action, i.e. y becomes independent of a , further implying that the second summand just acts as a constant (w.r.t. a) and can therefore be removed from Eq. 4. Therefore, in presence of counterfactual evidence, the Bellman equation becomes

$$V^*(b_t) = \max_a \sum_r b_t(r|a) r. \quad (5)$$

Mapping Bayesian inference to Q -learning

In order for Bayesian inference and Q -learning to be comparable, we need to be able to treat the two formulations in an equal setting, i.e. draw a correspondence between Q -learning (Eq. 1) and Bayesian inference (Eqs. 4,5). We notice that the action chosen in the Q -learning paradigm is a softmax of the two Q -values, suggesting that the Q values act as a prediction for the expected reward of the two arms. Additionally, as the Q -values always stay in the interval $[0, 1]$, it seems appropriate to equate them to the estimates of immediate expected rewards p_i of the two arms.

Using the update rule for b_t (Eq. 3), we can identify an similar update rule for $p_{i,t}^s$ as

$$p_{i,t+1}^s = \begin{cases} \frac{\alpha_{i,t} + 2}{\alpha_{i,t} + \beta_{i,t} + 3}, & \text{if } a_t = i, r_t = 1, \\ \frac{\alpha_{i,t} + 1}{\alpha_{i,t} + \beta_{i,t} + 3}, & \text{if } a_t = i, r_t = 0, \\ \frac{\alpha_{i,t} + 1}{\alpha_{i,t} + \beta_{i,t} + 2}, & \text{if } a_t \neq i. \end{cases}$$

Given that we map $p_{i,t}^s$ to Q_t^v , let us re-write the above evolution equation in a manner similar to Eq. 1. We then write

$$p_{v,t+1}^s = p_{v,t}^s + \begin{cases} \alpha_+^v \cdot (r_t^v - p_{v,t}^s), & \text{if } (r_t^v = 1), \\ \alpha_-^v \cdot (r_t^v - p_{v,t}^s), & \text{if } (r_t^v = 0). \end{cases} \quad (6)$$

³Here we tacitly identify the belief distribution with the parameters of the belief distribution.

⁴This is also known in the literature as a (special case of) Bayes Adaptive Markov Decision Process (BAMDP) Duff [2002].

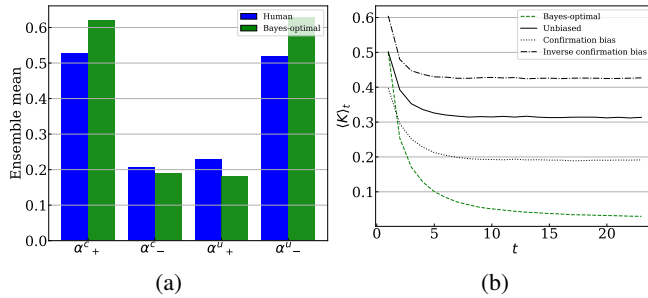


Figure 1: (a) Ensemble averaged best fit learning rates when fit to human data Palminteri et al. [2017] (blue) and Bayes-optimal agents (green). (b) Ensemble averaged action switching rates $\langle K \rangle_t$ as a function of time for Q -learning algorithms (black), humans (blue) and Bayes-optimal policy (green).

This implies that $\alpha_+ = \frac{p_{v,t+1}^s - p_{v,t}^s}{1 - p_{v,t}^s}$ where $p_{v,t+1}^s$ is given by the update rule with $r_t = 1$ and $\alpha_- = \frac{p_{v,t+1}^s - p_{v,t}^s}{-p_{v,t}^s}$ with $p_{v,t}^s$ is given by the update rule with $r_t = 0$. Upon making this substitution we find that

$$\alpha_{\pm} = \frac{1}{\alpha_{v,t} + \beta_{v,t} + 3} = \frac{1}{t + 3}. \quad (7)$$

This result is of fundamental importance. We have established that Bayesian inference can be precisely mapped onto a Q -learning formulation with no inherent bias (i.e., $\alpha_+^v = \alpha_-^v$)⁵. Given this, the findings from the model-fitting procedure in Fig. 1(a) present a significant conceptual challenge. The behavioral data are generated from an unbiased algorithm—Bayesian inference with optimal decision-making—yet, when fitting the Q -learning model (Eq. 1) to this data, the inferred learning rates exhibit asymmetry, suggestive of bias.

This discrepancy suggests that the source of the observed biases does not lie in the underlying decision process itself but rather in the structure of the model used to analyze it. Specifically, while Bayesian inference follows a learning rate that decreases monotonically as $\sim \frac{1}{t}$ (where t denotes the number of pulls), the standard Q -learning framework assumes a constant learning rate. As a result, when fitting Q -learning to Bayesian-generated data, the failure to account for this temporal dependence leads to the systematic misestimation of learning rates, introducing spurious asymmetries. In the following section, we provide a formal analysis of this phenomenon and its implications for modeling human decision-making.

2 Explaining the observation

With the correspondence between Q -learning and Bayes-greedy agents in place, we can now begin to compare the two Q -learning algorithms. More specifically we ask the question - when fitting stationary learning rates (from Eq. 1) to data generated by Eq. 7, why do we observe a confirmation/positivity bias? Further, as both positivity and confirmation biases are observed in TABB tasks with counterfactual information, we will perform our analysis only for that setting. A similar analysis can be performed for the case without counterfactual evidence.

We will argue that the answer lies in the dynamics of action switching probabilities implied by the two algorithms (see Fig. 1 (b)). More specifically, we will show that, when starting from constant and unbiased learning rates, there are two distinct ways of reducing the action switching rates - either by introducing a (positivity/confirmation) bias and keeping the learning rates constant or by maintaining unbiasedness in the learning rates but decreasing them monotonically with time⁶.

⁵This result holds specifically for Bernoulli bandits; although an analogous derivation applies to Gaussian bandits under a Gaussian prior. More general relationships between Bayesian inference and Q -learning in broader settings remain an open question.

⁶Not all temporal protocols lead to a decrease in action switching rates.

Therefore, we begin by first exploring the effects of biases on action switching rates, then followed by temporally varying learning rates. Finally, as the action switching rates also depend on the reward statistics of the environment, we consider symmetric environments i.e. $(p_1, p_2) = (p, p)$. This not only simplifies the analytical calculations but also allows us the study the exclusive effects of biases on action switching rates.

2.1 Action switching under constant learning rates

We now start with the Q -learning algorithm from Eq. 1, where the agent is described by the parameters $(\{\alpha_{\pm}^v\}, \beta)$. Eq. 1 is a stochastic difference equation (SDE) governing the time evolution $\mathbf{Q} = (Q_1, Q_2)$. Obtaining relevant quantities of interest would require us to perform multiple simulation runs (for averaging) of the Q -learning algorithm. This becomes particularly problematic if we are to explore a high dimensional parameter space (five dimensional system from Eq. 1). Alternatively, we could directly consider the time evolution of the probability distribution $P(\mathbf{Q})$ over the Q -values, via what is called a *master equation* Gardiner [1985]. This allows us to consider the time evolution of a deterministic system, and also allows further analytical treatment.

We denote the distribution at time t by $P_t(\cdot)$ and therefore write the master equation as

$$P_{t+1}(\mathbf{Q}) = \int P_t(\mathbf{Q}') \mathcal{T}(\mathbf{Q}' \rightarrow \mathbf{Q}; \{\alpha_{\pm}^v\}) d\mathbf{Q}', \quad (8)$$

where \mathcal{T} denotes the transition kernel of the stochastic process. In our case, $\mathcal{T}(\mathbf{Q}' \rightarrow \mathbf{Q}; \{\alpha_{\pm}^v\})$ is given by

$$\mathcal{T}(\mathbf{Q}' \rightarrow \mathbf{Q}; \{\alpha_{\pm}^v\}) = \sum_i \pi_i(\mathbf{Q}') \mathcal{T}_{-i}(Q_{-i}, Q'_{-i}; \alpha_{\pm}^u) \mathcal{T}_i(Q_i, Q'_i; \alpha_{\pm}^c), \quad (9)$$

where π_i is the probability of taking action i , $\mathcal{T}_{-i} \equiv p\delta(Q_{-i} - Q'_{-i} - \alpha_{+}^u(1 - Q'_{-i})) + (1 - p)\delta(Q_{-i} - Q'_{-i} + \alpha_{-}^u Q'_{-i})$ and $\mathcal{T}_i \equiv p\delta(Q_i - Q'_i - \alpha_{+}^c(1 - Q'_i)) + (1 - p)\delta(Q_i - Q'_i + \alpha_{-}^c Q'_i)$. Here the product $\mathcal{T}_{-i} \mathcal{T}_i$ reflects the assumption of independent rewards for both the arms and the specific forms reflect the update rules given by Eq. 1 with the reward probabilities $(p_1, p_2) = (p, p)$ as aforementioned.

We are interested in the total probability of switching the action under a 1-step transition from the state \mathbf{Q}' . In order to obtain that we first write the action switching probability under a specific transition $\mathbf{Q}' \rightarrow \mathbf{Q}$, which we represent by $K(\mathbf{Q}' \rightarrow \mathbf{Q}; \{\alpha_{\pm}^v\})$ and is given by $K(\mathbf{Q}' \rightarrow \mathbf{Q}; \{\alpha_{\pm}^v\}) = \sum_i \pi_i(\mathbf{Q}') (1 - \pi_i(\mathbf{Q})) \mathcal{T}_{-i}(Q_{-i}, Q'_{-i}; \alpha_{\pm}^u) \mathcal{T}_i(Q_i, Q'_i; \alpha_{\pm}^c)$. The total probability of action switching is then obtained by marginalising over the future states \mathbf{Q} and is given by

$$K(\mathbf{Q}'; \{\alpha_{\pm}^v\}) = \sum_i \pi_i(\mathbf{Q}') \int (1 - \pi_i(\mathbf{Q})) \mathcal{T}_{-i}(Q_{-i}, Q'_{-i}; \alpha_{\pm}^u) \mathcal{T}_i(Q_i, Q'_i; \alpha_{\pm}^c) d\mathbf{Q}. \quad (10)$$

The ensemble-average total probability of action switching at time t is then given by

$$\langle K \rangle_t = \int K(\mathbf{Q}; \{\alpha_{\pm}^v\}) P_t(\mathbf{Q}) d\mathbf{Q}. \quad (11)$$

We can obtain the time-evolution of the ensemble-average of a quantity $f(\mathbf{Q})$ as

$$\begin{aligned} \langle f \rangle_{t+1} &= \int f(\mathbf{Q}) P_{t+1}(\mathbf{Q}) d\mathbf{Q} \\ &= \int P_t(\mathbf{Q}') \int f(\mathbf{Q}) \mathcal{T}(\mathbf{Q}' \rightarrow \mathbf{Q}; \{\alpha_{\pm}^v\}) d\mathbf{Q} d\mathbf{Q}' = \langle I \rangle_t, \end{aligned} \quad (12)$$

where $I = \int f(\mathbf{Q}) \mathcal{T}(\mathbf{Q}' \rightarrow \mathbf{Q}; \{\alpha_{\pm}^v\}) d\mathbf{Q}$. Making the substitution for \mathcal{T} we get

$$\begin{aligned} \langle f \rangle_{t+1} &= \langle p^2 f(Q_1^{+,u}, Q_2^{+,c}) + p(1-p)f(Q_1^{-,u}, Q_2^{+,c}) \\ &\quad + p(1-p)f(Q_1^{+,u}, Q_2^{-,c}) + (1-p)^2 f(Q_1^{-,u}, Q_2^{-,c}) \rangle_t \\ &\quad + \langle \pi[p^2 f(Q_1^{+,c}, Q_2^{+,u}) + p(1-p)f(Q_1^{-,c}, Q_2^{+,u}) \\ &\quad + p(1-p)f(Q_1^{+,c}, Q_2^{-,u}) + (1-p)^2 f(Q_1^{-,c}, Q_2^{-,u}) \\ &\quad - p^2 f(Q_1^{+,u}, Q_2^{+,c}) - p(1-p)f(Q_1^{-,u}, Q_2^{+,c}) \\ &\quad - p(1-p)f(Q_1^{+,u}, Q_2^{-,c}) - (1-p)^2 f(Q_1^{-,u}, Q_2^{-,c})] \rangle_t, \end{aligned} \quad (13)$$

and here we use the shorthand $Q_i^{+,v} = Q_i + \alpha_+^v(1 - Q_i)$ and $Q_i^{-,v} = Q_i - \alpha_-^v Q_i$. As we are dealing with symmetric environments we have $\langle f(Q_1, Q_2) \rangle = \langle f(Q_2, Q_1) \rangle$. Therefore, by making use of Eq. 12 we can obtain the time evolution equations for the first two moments of $P(Q_1, Q_2)$ as follows. For the mean $\langle Q_1 \rangle$ we have

$$\langle Q_1 \rangle_{t+1} = B_1^{(1)} \langle Q_1 \rangle_t + B_1^{(2)} \langle \pi Q_1 \rangle_t + B^{(1)}. \quad (14)$$

Here, $B_1^{(1)} = p^2(1 - \alpha_+^u) + (1 - p)^2(1 - \alpha_-^u) + p(1 - p)(2 - \alpha_+^u - \alpha_-^u)$, $B_1^{(2)} = p^2(\alpha_+^u - \alpha_+^c) + (1 - p)^2(\alpha_-^u - \alpha_-^c) + p(1 - p)(\alpha_+^u + \alpha_-^u - \alpha_-^c - \alpha_+^c)$, $B^{(2)} = p(\alpha_+^c - \alpha_+^u)$ and $B^{(1)} = p\alpha_+^u$. Similarly $\langle Q_1 Q_2 \rangle$ evolves according to

$$\begin{aligned} \langle Q_1 Q_2 \rangle_{t+1} = & \left[C_{12}^{(1)} \langle Q_1 Q_2 \rangle_t + C_1^{(1)} \langle Q_1 \rangle_t + C_2^{(1)} \langle Q_2 \rangle_t + C^{(1)} \right] + \\ & \left[(C_{12}^{(2)} - C_{12}^{(1)}) \langle \pi Q_1 Q_2 \rangle_t + (C_1^{(2)} - C_1^{(1)}) \langle \pi Q_1 \rangle_t + \right. \\ & \left. (C_2^{(2)} - C_2^{(1)}) \langle \pi Q_2 \rangle_t + (C^{(2)} - C^{(1)}) \langle \pi \rangle_t \right]. \end{aligned} \quad (15)$$

Here $C_{12}^{(1)} = p^2(1 - \alpha_+^u)(1 - \alpha_+^c) + p(1 - p)[(1 - \alpha_-^u)(1 - \alpha_+^c) + (1 - \alpha_+^u)(1 - \alpha_-^c)] + (1 - p)^2(1 - \alpha_-^u)(1 - \alpha_-^c) = C_{12}^{(2)}$, $C_1^{(1)} = \alpha_+^c(1 - \alpha_+^u)p^2 + \alpha_+^c(1 - \alpha_-^u)(1 - p)p = C_2^{(2)}$, $C_2^{(1)} = \alpha_+^u(1 - \alpha_+^c)p^2 + \alpha_+^u(1 - \alpha_-^c)(1 - p)p = C_1^{(2)}$ and $C^{(1)} = p^2\alpha_+^c\alpha_+^u = C^{(2)}$. Using the relationships between these constants and also making use of the symmetry relations - $\langle \pi Q_1 \rangle = \langle (1 - \pi)Q_2 \rangle$ and $\langle Q_1 \rangle = \langle Q_2 \rangle$ we can simplify the above expression to

$$\begin{aligned} \langle Q_1 Q_2 \rangle_{t+1} = & C_{12}^{(1)} \langle Q_1 Q_2 \rangle_t + (C_1^{(1)} + C_2^{(1)}) \langle Q_1 \rangle_t \\ & + C^{(1)} + (C_2^{(1)} - C_1^{(1)}) \left[2\langle \pi Q_1 \rangle_t - \langle Q_1 \rangle_t \right]. \end{aligned} \quad (16)$$

Finally $\langle Q_1^2 \rangle$ evolves according to

$$\begin{aligned} \langle Q_1^2 \rangle_{t+1} = & \left[D_{11}^{(1)} \langle Q_1^2 \rangle_t + D_1^{(1)} \langle Q_1 \rangle_t + D^{(1)} \right] \\ & + \left[(D_{11}^{(2)} - D_{11}^{(1)}) \langle \pi Q_1^2 \rangle_t + (D_1^{(2)} - D_1^{(1)}) \langle \pi Q_1 \rangle_t \right. \\ & \left. + (D^{(2)} - D^{(1)}) \langle \pi \rangle_t \right], \end{aligned} \quad (17)$$

where $D_{11}^{(1)} = p(1 - \alpha_+^u)^2 + (1 - p)(1 - \alpha_-^u)^2$, $D_1^{(1)} = 2p\alpha_+^u(1 - \alpha_+^u)$, $D^{(1)} = p(\alpha_+^u)^2$ and the corresponding $D^{(2)}$ terms are the same, except that \cdot^u is replaced with \cdot^c .

The above three deterministic difference equations in Eqs. 14, 16 and 17 govern the time evolution of the first two moments of the joint probability distribution over the Q-values. However, they require us to know the integrals for $\langle \pi \rangle_t$, $\langle \pi Q_1 \rangle_t$ and $\langle \pi Q_1^2 \rangle_t$. Generally speaking, evaluating these integrals in closed form is only possible in very simplified scenarios and sadly Eq. 8 doesn't fall in that category. One can however, recall the standard textbook knowledge (Benaroya et al. [2005]) that the mean of some (non-linear) transformation (in our case f) of a random variable (\mathbf{Q} in our case) can be approximated by transformations of the moments of the random variable. This should simplify our lives and allow us to approximate the integrals above and consequently provide us with (approximate) deterministic dynamics for $\langle f \rangle_t$ which would be amenable to deeper analytical treatment in comparison to stochastic difference equations as in Eq. 1. The approximation can be derived as follows.

$$\int f(\mathbf{Q}) P_t(\mathbf{Q}) d\mathbf{Q} = \int f(\boldsymbol{\mu}_Q + (\mathbf{Q} - \boldsymbol{\mu}_Q)) P_t(\mathbf{Q}) d\mathbf{Q}. \quad (18)$$

If f is a smooth function, we can Taylor expand it around $\boldsymbol{\mu}_Q = (\langle Q_1 \rangle, \langle Q_2 \rangle)$ upto second order gives,

$$\begin{aligned} f(\boldsymbol{\mu}_Q + (\mathbf{Q} - \boldsymbol{\mu}_Q)) \approx & f(\boldsymbol{\mu}_Q) + \nabla f(\boldsymbol{\mu}_Q) \cdot (\mathbf{Q} - \boldsymbol{\mu}_Q) \\ & + \frac{1}{2!} (\mathbf{Q} - \boldsymbol{\mu}_Q)^T H_f(\mathbf{Q} - \boldsymbol{\mu}_Q) \\ & + \mathcal{O}((\mathbf{Q} - \boldsymbol{\mu}_Q)^3), \end{aligned} \quad (19)$$

where H_f is the Hessian matrix of f . Finally, performing the integral over this approximation of f then allows us to write

$$\langle f \rangle_t \approx f(\boldsymbol{\mu}_Q) + \frac{1}{2} H_{f,ij} \langle (Q_i - \mu_i)(Q_j - \mu_j) \rangle_t, \quad (20)$$

where we've used the Einstein summation convention. Eq. 20 finally allows us to approximate the mean of a non-linear transformation f in terms of mean and covariance matrices of \boldsymbol{Q} . We can make use of this approximation to now write down the integrals $\langle \pi \rangle_t$, $\langle \pi Q_1 \rangle_t$ and $\langle \pi Q_1^2 \rangle_t$ in terms of $\langle Q_1 \rangle_t$, $\langle Q_1 Q_2 \rangle_t$ and $\langle Q_1^2 \rangle_t$, the evolution equations of which are have already been obtained in Eqs. 14, 16 and 17 respectively.

We begin by evaluating $\langle \pi \rangle_t$. Making use of the functional form of $\pi(\boldsymbol{Q}) = \frac{1}{1+e^{-\beta(Q_1-Q_2)}}$ we can obtain its Hessian matrix to be

$$H_\pi = \beta^2 \pi(1-\pi)(1-2\pi) \begin{pmatrix} 1 & -1 \\ -1 & 1 \end{pmatrix}. \quad (21)$$

Recalling the symmetry in our system we have $\langle Q_1 \rangle_t = \langle Q_2 \rangle_t$, implying that $\pi(\boldsymbol{\mu}_Q) = \frac{1}{2}$ and therefore $H_\pi = \mathbf{0}$, making the second term vanish. This finally implies $\langle \pi \rangle_t = \frac{1}{2}$.

For $\langle \pi Q_1 \rangle_t$ we need to evaluate the Hessian matrix $H_{\pi Q_1}$, which evaluates to

$$H_{\pi Q_1} = \beta \pi(1-\pi) \begin{pmatrix} 2 + \beta Q_1(1-2\pi) & -1 - \beta Q_1(1-2\pi) \\ -1 - \beta Q_1(1-2\pi) & \beta Q_1(1-2\pi) \end{pmatrix}, \quad (22)$$

which under the symmetry condition evaluates to

$$H_{\pi Q_1} = \frac{\beta}{4} \begin{pmatrix} 2 & -1 \\ -1 & 0 \end{pmatrix}. \quad (23)$$

Making use of this we obtain the approximation for $\langle \pi Q_1 \rangle_t$ to be

$$\langle \pi Q_1 \rangle_t = \frac{\langle Q_1 \rangle_t}{2} + \frac{\beta}{4} (\langle Q_1^2 \rangle_t - \langle Q_1 Q_2 \rangle_t) \quad (24)$$

Finally, $H_{\pi Q_1^2}$ evaluates to

$$H_{\pi Q_1^2} = \pi \begin{bmatrix} 2 + 2\beta Q_1(1-\pi) + \beta(1-\pi) & -\beta(1-\pi)(2Q_1+ \\ (2Q_1 + \beta Q_1^2(1-2\pi)) & \beta Q_1^2(1-2\pi) \\ -\beta(1-\pi)(2Q_1+ \\ \beta Q_1^2(1-2\pi)) & \beta Q_1^2(1-\pi)(1-2\pi) \end{bmatrix} \quad (25)$$

which under the symmetry condition evaluates to

$$H_{\pi Q_1^2} = \begin{pmatrix} 1 + \beta Q_1 & -\frac{\beta}{2} Q_1 \\ -\frac{\beta}{2} Q_1 & 0 \end{pmatrix}. \quad (26)$$

This gives us approximation

$$\langle \pi Q_1^2 \rangle_t = \frac{\langle Q_1^2 \rangle_t}{2} + \frac{\beta}{2} \langle Q_1 \rangle_t (\langle Q_1^2 \rangle_t - \langle Q_1 Q_2 \rangle_t). \quad (27)$$

We can now substitute these approximations into Eqs. 14, 16 and 17 to obtain the closed-form (approximate) dynamics for the first two moments to be

$$\langle Q_1 \rangle_{t+1} = \left(B_1^{(1)} + \frac{B_1^{(2)}}{2} \right) \langle Q_1 \rangle_t + \frac{B_1^{(2)} \beta}{4} \Delta_t + B^{(1)} + \frac{B^{(2)}}{2}. \quad (28a)$$

$$\begin{aligned} \langle Q_1 Q_2 \rangle_{t+1} = & C_{12}^{(1)} \langle Q_1 Q_2 \rangle_t + (C_1^{(1)} + C_2^{(1)}) \langle Q_1 \rangle_t \\ & + C^{(1)} + (C_2^{(1)} - C_1^{(1)}) \frac{\beta}{2} \Delta_t, \end{aligned} \quad (28b)$$

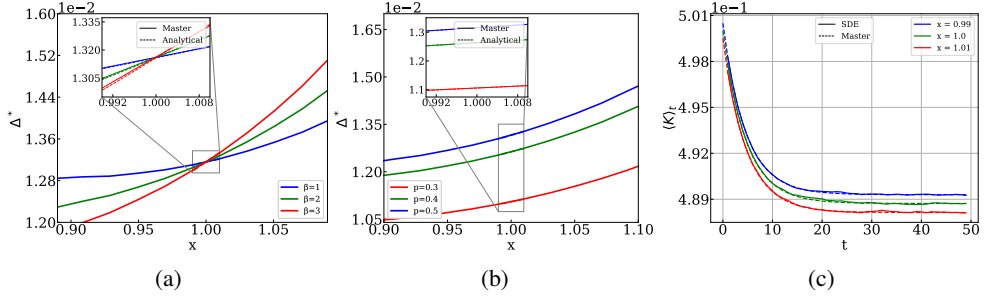


Figure 2: Steady state Δ^* as a function of confirmation bias x , for different values of (a) β and (b) p values. (c) shows the average action switching probability $\langle K \rangle_t$ as a function of t , for different values of confirmation bias.

$$\begin{aligned} \langle Q_1^2 \rangle_{t+1} = & \left[\frac{(D_{11}^{(2)} + D_{11}^{(1)})}{2} \langle Q_1^2 \rangle_t + \frac{(D_1^{(2)} + D_1^{(1)})}{2} \langle Q_1 \rangle_t + D^{(1)} \right] \\ & + \left[(D_{11}^{(2)} - D_{11}^{(1)}) \langle Q_1 \rangle_t \frac{\beta}{2} \Delta_t \right. \\ & \left. + (D_1^{(2)} - D_1^{(1)}) \frac{\beta}{4} \Delta_t + \frac{(D^{(2)} - D^{(1)})}{2} \right], \end{aligned} \quad (28c)$$

Here we write $\langle \frac{(Q_1 - Q_2)^2}{2} \rangle_t = \langle Q_1^2 \rangle_t - \langle Q_1 Q_2 \rangle_t = \Delta_t$.

With the approximate solution of the master equation in place, we are now prepared to comment on the time evolution of $\langle K \rangle_t$. Instead of going from the route of Eq. 20 which would be cumbersome, we start by first taking a closer look at the form of K from Eq. 10. Some simple algebra reveals that K is monotonically decreasing in $\sqrt{2\Delta} = |Q_1 - Q_2|, \alpha_+^c, \alpha_-^u$ and monotonically increasing in α_-^c, α_+^u . Intuitively, as the Q values go far apart, the probability of switching the action in just one time-step is lower. Similarly, higher values of α_+^c, α_-^u drive the Q values of the chosen and the unchosen options further apart (as the chosen option is more likely going to be the bigger of the Q values), thereby decreasing the action switching probability. And an opposite effect is to be expected for α_-^c, α_+^u . As we wish to look for the effect of constant learning rates on the temporal evolution of $\langle K \rangle_t$, the temporal variation is only going to come via the (temporal-)variation in Δ_t . We can already make use of Eqs. 28 to find the time evolution of Δ_t and more specifically look at the steady state value Δ^* and note how it varies with confirmation bias.

We solve for the steady state the system of equations in Eq. 28 and obtain a quadratic equation in Δ^* . Upon taking the derivative of Δ^* with respect to the normalized confirmation bias⁷ $C = \frac{\alpha_+^c - \alpha_-^c - \alpha_+^u + \alpha_-^u}{\alpha_+^c + \alpha_-^c + \alpha_+^u + \alpha_-^u}$, we obtain that $\frac{\partial \Delta^*}{\partial C} > 0$ as long as $p(1 - p) \neq 0$. This confirms our intuitions Palminteri et al. [2017], Lefebvre et al. [2022] that confirmation bias leads to larger differences between the Q values of the arms and therefore decreases the action switching probabilities. We are further able to note that $\frac{\partial^2 \Delta^*}{\partial \beta \partial C} > 0$, therefore implying that increasing the inverse temperature amplifies the effect of confirmation bias on the action switching probabilities. These trends can be seen in Fig. 2 (a,b) where we see Δ^* as a function of x ⁸. In the figure $x = 1$ represents unbiased learning rates and we have confirmation bias for $x > 1$. We also note that for $x = 1$, in Fig. 2 (a), the curves for all values of β intersect at the same point. This is because for symmetric learning rates, the learning dynamics become decoupled from the action selection. This can also be seen from the analytical expressions in Eqs. 28 by setting $\alpha_{\pm}^u = \alpha$. In particular, as Bayesian inference is unbiased we see that in Eqs. 29, there is no dependence on action selection *i.e.* β .

Nonetheless, we can conclude that introduction of a confirmation bias increases Δ^* thereby leading to lower $\langle K \rangle_t$ as can be seen in Fig. 2 (c).

⁷As proposed in Palminteri et al. [2017]

⁸We use x to parameterize a curve where $\alpha_+^c = \alpha_-^u = 0.1x$ and $\alpha_+^u = \alpha_-^c = 0.2 - 0.1x$, making $C = 2(x - 1)$.

2.2 Action switching under time-varying learning rates

Eqs. 28 are greatly simplified for the case of Bayesian inference, as $\alpha_{\pm}^v = \alpha_t = \frac{1}{t+3}$. Making the appropriate substitutions, we obtain the following set of evolution laws.

$$\langle Q_1 \rangle_{t+1} = (1 - \alpha_t) \langle Q_1 \rangle_t + p \alpha_t, \quad (29a)$$

$$\langle Q_1 Q_2 \rangle_{t+1} = (1 - \alpha_t)^2 \langle Q_1 Q_2 \rangle_t + 2p \alpha_t (1 - \alpha_t) \langle Q_1 \rangle_t + p^2 \alpha_t^2, \quad (29b)$$

$$\langle Q_1^2 \rangle_{t+1} = (1 - \alpha_t)^2 \langle Q_1^2 \rangle_t + 2p \alpha_t (1 - \alpha_t) \langle Q_1 \rangle_t + p \alpha_t^2. \quad (29c)$$

These evolution laws imply that Δ_t evolves according to

$$\Delta_{t+1} = \underbrace{(1 - \alpha_t)^2 \Delta_t}_{\text{epistemic drift}} + \underbrace{p(1 - p) \alpha_t^2}_{\text{noise}}, \quad (30)$$

where $\alpha_t = \frac{1}{t+3}$ as seen in Eq. 7. From Eq. 30 is particularly insightful as one can identify two distinct components to the time evolution of Δ_t : a drift term and a second noise driven term. We take note that the drift term has a coefficient $(1 - \alpha_t)^2 \leq 1$, implying that the drift always tries to drive Δ_t to zero. This makes sense, as we are dealing with symmetric environments and Bayesian inference indeed converges to the truth asymptotically i.e. $\Delta_{\infty} = 0$. The noise driven term is proportional to the variance of the environment $p(1 - p)$ which drives Δ_t to larger values (proportional to α_t^2). This allows us to guess how Bayesian inference sustains low $\langle K \rangle_t$ for the time-scales observed in experiments - in the small time regime because we start from $\Delta_0 = 0$, the drift term is small compared to the noise term. Therefore, random fluctuations of the environment drive the Q values apart, decreasing the action switching rates. But at slightly larger times, the noise term becomes insignificant as it is quadratic in α_t and the drift term is linear in α_t . This implies that Δ_t starts reducing, albeit at a very small rate, because for small α_t , $(1 - \alpha_t)^2$ is close to unity. In totality, Bayes inference maintains low action switching rates, by first driving the Δ_t to higher values by environmental fluctuations, and then by decreasing the learning rates such that the Q values become "sluggish", thereby sustaining the low action switching rates.

We now make the above arguments quantitatively precise, by considering the time-scales in the system. First, we notice that for a stationary $\alpha_t = \alpha$, Δ relaxes to the steady state with a time-scale $\tau = \frac{1}{\alpha(2-\alpha)}$ and the steady state is given by $\Delta^* = \frac{p(1-p)\alpha}{(2-\alpha)}$. As $\alpha \in [0, 1]$, Δ^* is increasing in α . Additionally, K is monotonically increasing in α . This suggests that in order to obtain low $\langle K \rangle$ by modulating α_t alone, one first starts with a relatively large value for α and keep the value large for times comparable to τ^9 . This will lead the system to have large Δ_t . Once the Δ equilibrates, decrease α_t rapidly, thereby leading to small $\langle K \rangle_t$. Such a temporal protocol can sustain low action switching probabilities for relatively long times as τ is large for very small α and therefore Δ will decrease over a slow time-scale. For the purpose of demonstration we choose

$$\alpha_t = \begin{cases} \alpha_1, & t < \tau_c \\ \alpha_2, & t \geq \tau_c, \end{cases}$$

and observe the impact on $\langle K \rangle_t$ in Fig. 3. We are able to notice that $\langle K \rangle_t$ experiences a sudden drop at $\tau_c = 25$ and then slowly approaches (a higher) equilibrium corresponding to α_2 . In doing so, for an intermediate time the action switching rates are lower than the case with $\alpha_2 = \alpha_1$. The minimum $\langle K \rangle_t$ depends on the exact value of α_1 . More notably achieving the same $\langle K \rangle_{\min}$ is possible for smaller values of τ_c as α_1 increases, thereby confirming our intuitions arising from Eq. 29.

With the above arguments in place, it is relatively straightforward to see that we have identified two distinct routes to decreasing the action switching rates in bandit tasks. First, by introducing a bias in the learning rates. Second, by decreasing the learning rates with time, while being consistent with the arguments in Sec. 2.2. In conclusion we have answered the question we set out for at the beginning of this section.

⁹As τ is decreasing in α , this waiting period for large starting α_0 is relatively small, as is the case for Bayesian inference where $\alpha_0 = \frac{1}{3}$.

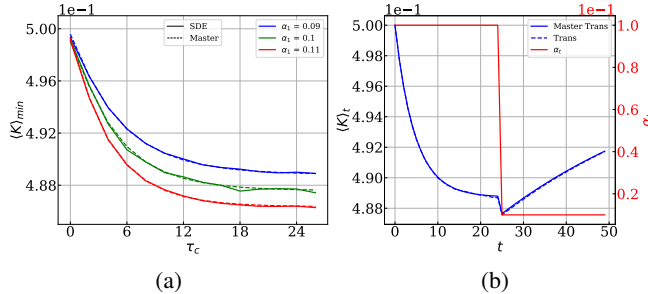


Figure 3: (a) The minimum (across time t) value of the average action switching rate $\langle K \rangle_{\min}$ as a function of τ_c for different values of α_1 . (b) α_t and the corresponding action switching rates $\langle K \rangle_t$ as a function for time for $\tau_c = 25$ and $\alpha_1, \alpha_2 = 0.1, 0.01$.

3 Consequences on human behavior

We have so far explored that both confirmation bias and Bayesian inference can lead to similar behavioral signatures. The confounding effects of Bayesian inference and confirmation bias leads us to a further question - how do we distinguish bias from optimal inference or a more general temporal profile of the learning rates? Before we even begin to attempt an answer, we first take a note of how well these models explain human behavior in stationary TABB tasks.

3.1 Model comparison

We proceed by comparing model fits to data from Palminteri et al. [2017]. When performing fits to data we consider, a Bayes-greedy model (Eq. 5, referred as "Bayes"), unbiased Q-learning model (Eq. 1 with $\alpha_{\pm} = \alpha$, referred as "Const.") and the full Q-learning model (Eq. 1, referred as "Full") and also a "confirmation model agent" (Eq. 1 with $\alpha_+^c = \alpha_-^u$ and $\alpha_-^c = \alpha_+^u$, referred as "Conf."). We keep the fitting procedure to be similar to that of Palminteri et al. [2017]- i.e. we minimize the negative log-likelihood of the models for each participant's data to find the best fit parameters. As the models vary in their complexities (degrees of freedom (represented as "df" in the following tables)), we obtain for each participating subject, the Bayesian information criterion (BIC) scores corresponding to each of the best-fit models. Table 1 shows the mean and standard deviations of the best fit negative log-likelihoods (NLL) and the BIC scores for each of the model for all the subjects.

In Fig. 4 (a) we present the average action switching rates for humans and the corresponding best

TABB with counterfactual information				
	Bayes (1df)	Full (5df)	Const. (2df)	Conf. (3df)
NLL	9.48 ± 6.21	6.14 ± 5.23	9.12 ± 6.29	6.89 ± 5.47
BIC	22.13 ± 12.43	28.17 ± 10.45	24.59 ± 12.57	23.31 ± 10.93

Table 1: NLL and BIC values

fit Bayesian and Q -learning agents (both biased and unbiased). It can be seen that the best fit Q -learners with unbiased and constant learning rates are unable to account for the low action switching rates observed in human data. However, both Bayesian and confirmation biased Q -learners are able to fit relatively well to human behavior.

Additionally, we report the proportion of best describing models in the subject population in Fig. 4 (b). We say that a subject is best described by a model i if it has the lowest BIC of all the other models. As can be seen from Fig. 4 (b), most subjects are best described by the Bayesian model, and quite expectedly by the "full" model if we ignore issues of model complexity. As aforementioned, we have followed suit with Palminteri et al. [2017] in so far as penalising model complexity is concerned, but we acknowledge that penalising complexity is not straightforward and therefore we do not take the above results to mean - "humans are Bayesian". However, these results suggest that if we account for temporally decreasing learning rates, we are likely to observe lower levels of confirmation bias as compared to when we do not account for it. In particular, behavior may

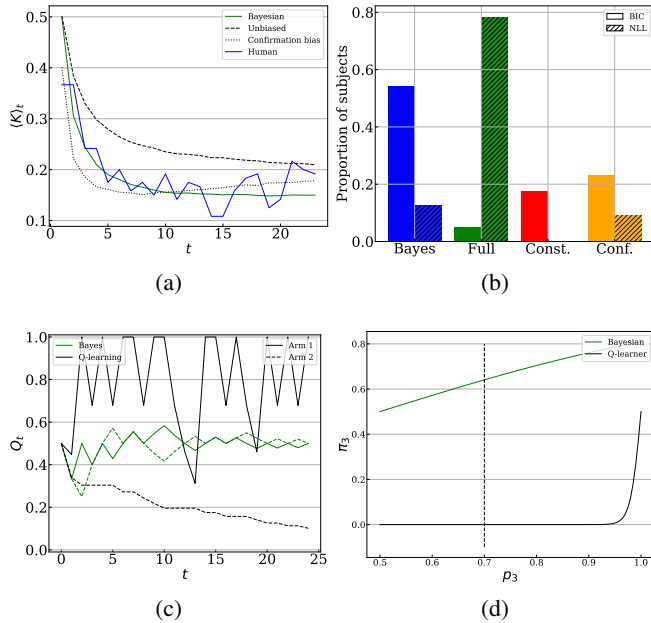


Figure 4: (a) Ensemble average action switching rates for human data (blue), best fit Bayesian agents (green), best fit Q -learning agents (black) for both unbiased (dashed) and biased (dotted) learning rates. (b) Distribution of best describing models for all human subjects by BIC (solid) scores and NLL (striped) scores. (c) Best fit Q -value trajectories for an exemplar human subject corresponding to Bayesian (green) and Q -learning model (black). (d) Probability of choosing the newly introduced arm as a function of its reward rate, for the best fit Bayesian (green) and Q -learning model (black).

be better described via hybrid models which have a combination of bias and temporally decreasing learning rates. Therefore, further investigation would be needed to disentangle Bayesian and biased models from human behavior in TABB tasks.

3.2 Potential empirical investigations

As we explored in Sec. 2.2, while both Bayesian and (confirmation) biased agents exhibit decreasing action switching rate $\langle K \rangle$, they do so via distinct mechanisms. Confirmation bias achieves low $\langle K \rangle$ by driving the system to larger Δ and Bayes inference achieves it by lowering $|\alpha_t|$. This suggests that on average the two mechanisms will lead to different steady state Q values. In Fig. 4(c) we compare the Q values obtained from the best fit Bayesian model and the best fit Q -learning model (at terminal time $t = 24$) for an example participant in a symmetric environment (i.e. $p = 0.5$). We see that our two guesses for human behavior imply very distinct Q -values. In particular we see that the Bayesian model predicts that the Q -values converge to the true reward rates p , while the Q -learning model drives the Q -values further apart.

In order to empirically distinguish between the Bayesian inference and biased Q -learning, one may, at the end of the task, introduce a new arm with a reward probability p_3 which lies in between the Bayesian and Q -learning best fit Q values for a given arm (say arm 1). The subject would have to be separately trained on the new arm and then asked to choose between the new arm and a given arm (arm 1), whether or not the player chooses the new arm might help distinguish between Bayesian and Q -learning agents. In Fig. 4 (d) we present the supposed probability of choosing the new arm (π_3) as a function of its reward rate p_3 for both the Bayesian and Q -learning model.

4 Discussion

This work present a rigorous theoretical comparison between Q -learning and Bayesian inference in TABB task with counterfactual information. We utilize our theoretical analysis to critique recent

experimental studies on human behavior in TABB tasks. In particular we demonstrate that certain temporal profiles (including that of Bayes inference) of unbiased learning rates may show the behavioral signatures similar to that of a biased learning algorithm. This analysis also sheds light on why recent studies [Lefebvre et al., 2022, Bergerot et al., 2024] observe that confirmation bias leads to better accumulated rewards in comparison to unbiased Q -learning, where they assume the constancy of learning rates.

While doing so, we've also demonstrated the usefulness of Master equation type formulations, commonly used in statistical physics, to study RL algorithms. An analysis similar to our steady state analysis, has been done already [Lefebvre et al., 2022] without using the master equations. However their approach only works for epsilon-greedy algorithm with temporally constant learning rates, while our methodology is applicable to more general RL algorithms. In addition, the presented approach allows us to study the temporal dynamics of these learning systems, which cannot be obtained from a steady state analysis.

In conclusion, we demonstrate that making claims about confirmation bias by fitting a Q -learning model as in Eq. 1 to behavior can be problematic. As this methodology has been employed by lot of studies in cognitive science literature, we believe that our analysis will allow cognitive scientists to make more nuanced and robust claims about confirmation bias when inferred from decision making tasks.

References

Stefano Palminteri, Germain Lefebvre, Emma J Kilford, and Sarah-Jayne Blakemore. Confirmation bias in human reinforcement learning: Evidence from counterfactual feedback processing. *PLoS computational biology*, 13(8):e1005684, 2017.

Germain Lefebvre, Maël Lebreton, Florent Meyniel, Sacha Bourgeois-Gironde, and Stefano Palminteri. Behavioural and neural characterization of optimistic reinforcement learning. *Nature Human Behaviour*, 1(4):0067, 3 2017. ISSN 2397-3374. doi: 10.1038/s41562-017-0067. URL <https://doi.org/10.1038/s41562-017-0067>.

Hanneke E.M. den Ouden, Nathaniel D. Daw, Guillén Fernandez, Joris A. Elshout, Mark Rijpkema, Martine Hoogman, Barbara Franke, and Roshan Cools. Dissociable effects of dopamine and serotonin on reversal learning. *Neuron*, 80(4):1090–1100, 2013. ISSN 0896-6273. doi: <https://doi.org/10.1016/j.neuron.2013.08.030>. URL <https://www.sciencedirect.com/science/article/pii/S0896627313007897>.

Michael J Frank, Ahmed A Moustafa, Heather M Haughey, Tim Curran, and Kent E Hutchison. Genetic triple dissociation reveals multiple roles for dopamine in reinforcement learning. *Proceedings of the National Academy of Sciences*, 104(41):16311–16316, 2007.

Valérian Chambon, Héloïse Théro, Marie Vidal, Henri Vandendriessche, Patrick Haggard, and Stefano Palminteri. Information about action outcomes differentially affects learning from self-determined versus imposed choices. *Nature Human Behaviour*, 4(10):1067–1079, 2020.

Liyu Xia, Sarah L Master, Maria K Eckstein, Beth Baribault, Ronald E Dahl, Linda Wilbrecht, and Anne Gabrielle Eva Collins. Modeling changes in probabilistic reinforcement learning during adolescence. *PLoS computational biology*, 17(7):e1008524, 2021.

Benedikt Herrmann, Christian Thöni, and Simon Gächter. Antisocial punishment across societies. *Science*, 319(5868):1362–1367, 2008. doi: 10.1126/science.1153808. URL <https://www.science.org/doi/abs/10.1126/science.1153808>.

Prakhar Godara, Tilman Diego Aléman, and Stephan Herminghaus. Bounded rational agents playing a public goods game. *Phys. Rev. E*, 105:024114, Feb 2022. doi: 10.1103/PhysRevE.105.024114. URL <https://link.aps.org/doi/10.1103/PhysRevE.105.024114>.

Prakhar Godara and Stephan Herminghaus. Bounded learning and planning in public goods games. *Phys. Rev. E*, 107:054140, May 2023. doi: 10.1103/PhysRevE.107.054140. URL <https://link.aps.org/doi/10.1103/PhysRevE.107.054140>.

Guangrong Wang, Jianbiao Li, Wenhua Wang, Xiaofei Niu, and Yue Wang. Confusion cannot explain cooperative behavior in public goods games. *Proceedings of the National Academy of Sciences*, 121(10):e2310109121, 2024. doi: 10.1073/pnas.2310109121. URL <https://www.pnas.org/doi/abs/10.1073/pnas.2310109121>.

James Andreoni and Rachel Croson. Partners versus strangers: Random rematching in public goods experiments. *Handbook of experimental economics results*, 1:776–783, 2008.

Mark Steyvers, Michael D. Lee, and Eric-Jan Wagenmakers. A bayesian analysis of human decision-making on bandit problems. *Journal of Mathematical Psychology*, 53(3):168–179, 2009. ISSN 0022-2496. doi: <https://doi.org/10.1016/j.jmp.2008.11.002>. URL <https://www.sciencedirect.com/science/article/pii/S0022249608001090>. Special Issue: Dynamic Decision Making.

Shunan Zhang and Angela J Yu. Forgetful bayes and myopic planning: Human learning and decision-making in a bandit setting. *Advances in neural information processing systems*, 26, 2013.

Robert C Wilson, Andra Geana, John M White, Elliot A Ludvig, and Jonathan D Cohen. Humans use directed and random exploration to solve the explore–exploit dilemma. *Journal of experimental psychology: General*, 143(6):2074, 2014.

Vanessa M. Brown, Michael N. Hallquist, Michael J. Frank, and Alexandre Y. Dombrovski. Humans adaptively resolve the explore-exploit dilemma under cognitive constraints: Evidence from a multi-armed bandit task. *Cognition*, 229:105233, 2022. ISSN 0010-0277. doi: <https://doi.org/10.1016/j.cognition.2022.105233>. URL <https://www.sciencedirect.com/science/article/pii/S0010027722002219>.

Charley M Wu, Eric Schulz, Timothy J Pleskac, and Maarten Speekenbrink. Time pressure changes how people explore and respond to uncertainty. *Scientific reports*, 12(1):4122, 2022.

Michael N. Katehakis and Arthur F. Veinott. The multi-armed bandit problem: Decomposition and computation. *Mathematics of Operations Research*, 12(2):262–268, 1987. doi: 10.1287/moor.12.2.262. URL <https://doi.org/10.1287/moor.12.2.262>.

Hiroyuki Ohta, Kuniaki Satori, Yu Takarada, Masashi Arake, Toshiaki Ishizuka, Yuji Morimoto, and Tatsuji Takahashi. The asymmetric learning rates of murine exploratory behavior in sparse reward environments. *Neural Networks*, 143:218–229, 2021. ISSN 0893-6080. doi: <https://doi.org/10.1016/j.neunet.2021.05.030>. URL <https://www.sciencedirect.com/science/article/pii/S0893608021002264>.

Shiva Farashahi, Christopher H Donahue, Benjamin Y Hayden, Daeyeol Lee, and Alireza Soltani. Flexible combination of reward information across primates. *Nature human behaviour*, 3(11):1215–1224, 2019.

Peter Dayan and Laurence F Abbott. *Theoretical neuroscience: computational and mathematical modeling of neural systems*. MIT press, 2005.

Arnold Zellner. Optimal information processing and bayes’s theorem. *The American Statistician*, 42(4):278–280, 1988.

Dileep George and Jeff Hawkins. Towards a mathematical theory of cortical micro-circuits. *PLOS Computational Biology*, 5(10):1–26, 10 2009. doi: 10.1371/journal.pcbi.1000532. URL <https://doi.org/10.1371/journal.pcbi.1000532>.

Thomas L Griffiths, Charles Kemp, and Joshua B Tenenbaum. Bayesian models of cognition. 2008.

Kentaro Katahira. The statistical structures of reinforcement learning with asymmetric value updates. *Journal of Mathematical Psychology*, 87:31–45, 2018. ISSN 0022-2496. doi: <https://doi.org/10.1016/j.jmp.2018.09.002>. URL <https://www.sciencedirect.com/science/article/pii/S0022249617302407>.

Crispin W Gardiner. Handbook of stochastic methods for physics, chemistry and the natural sciences. *Springer series in synergetics*, 1985.

Michael O’Gordon Duff. *Optimal Learning: Computational procedures for Bayes-adaptive Markov decision processes*. University of Massachusetts Amherst, 2002.

Haym Benaroya, Seon Mi Han, and Mark Nagurka. *Probability models in engineering and science*, volume 192. CRC press, 2005.

Germain Lefebvre, Christopher Summerfield, and Rafal Bogacz. A Normative Account of Confirmation Bias During Reinforcement Learning. *Neural Computation*, 34(2):307–337, 01 2022. ISSN 0899-7667. doi: 10.1162/neco_a_01455. URL https://doi.org/10.1162/neco_a_01455.

Clémence Bergerot, Wolfram Barfuss, and Paweł Romanczuk. Moderate confirmation bias enhances decision-making in groups of reinforcement-learning agents. *PLOS Computational Biology*, 20(9):1–22, 09 2024. doi: 10.1371/journal.pcbi.1012404. URL <https://doi.org/10.1371/journal.pcbi.1012404>.